WILEY | Hindawi

Research Article

Interaction and Binding Kinetics of Different Substituted Pyrazines with HSA: Based on Multispectral, Physiological Activity, and Molecular Dynamics Simulations

Wenhua Tong [1,2,3] **Shuqin Wang,** [1] **Haoran Xu,** [1] **Zongwei Qiao,** [3] **Liming Zhao,** [4] **and Ying Yang** [1]

[1]*School of Biological Engineering, Sichuan University of Science and Engineering, Yibin 644000, Sichuan, China*
[2]*Liquor Brewing Biotechnology and Application Key Laboratory of Sichuan Province, Yibin 644000, Sichuan, China*
[3]*Sichuan Yibin Wuliangye Group Co., Ltd., Yibin 644007, Sichuan, China*
[4]*East China University of Science and Technology, Shanghai 200000, China*

Correspondence should be addressed to Wenhua Tong; tongwh@suse.edu.cn

Pyrazine is a kind of compound containing pyrazine ring structure, which has attracted the attention of researchers because of its special aroma and healthcare function. It is currently used in spices, pharmaceuticals, food additives, and other industries. Human serum albumin (HSA) is a transport and storage protein in the human circulatory system. Previous research reported that pyrazine can interact with albumin, but the interaction between pyrazine and HSA has not been reported. Consequently, this study is based on the multispectral method and molecular dynamics (MD) simulation, exploring the interaction between different pyrazines and HSA. The results show that the four pyrazines mainly quench the endogenous fluorescence of HSA through the static quenching mechanism. Molecular docking indicates that hydrophobic forces play a major role in the binding of pyrazines with HSA. At the same time, synchronous fluorescence spectroscopy, circular dichroism (CD), three-dimensional fluorescence spectroscopy, and resonance light scattering (RLS) showed that each pyrazine compound can change the conformation of HSA. MD simulation results show that the combination of four pyrazines and HSA can enhance the stability of HSA. Among them, 2,3,5,6-tetramethylpyrazine (TTMP) and 2,3,5-trimethylpyrazine (TMTP) binding is the most stable and the most unstable combination with HSA, respectively. In addition, the four pyrazines could affect the physiological activity of HSA. This study is of great significance to explore the mechanism of action of pyrazine compounds *in vivo* and can provide useful information for the application of pyrazine compounds in food.

1. Introduction

Human serum albumin (HSA) is a highly water-soluble spherical monomeric plasma protein, which has a variety of important functions and roles in the body. HSA can delay the metabolism or excretion of lipophilic substances in the human body and increase their solubility and half-life in plasma [1]. And it has been used as a biopharmaceutical in the clinical treatment of low blood volume, bleeding, shock, trauma, burns, and other diseases [2]. After some small drug molecules enter the human blood system, they reversibly bind to HSA before being stored and transported to exert their pharmacological effects [3, 4]. In addition, HSA also has the functions of osmotic adjustment, immune regulation, and maintaining acid-base balance [5, 6]. Therefore, HSA is widely used as a model protein for the study of protein structure.

Pyrazine is a kind of compound containing a pyrazine ring structure, which is widely found in nature, and can be utilized by microorganisms, plants, animals, and humans [7]. Currently, pyrazine and its derivatives are widely used in the spice, pharmaceutical, and food additive industries [8, 9].

2,3-Dimethylpyrazine (2,3-DMTP), 2,5-dimethylpyrazine (2,5-DMTP), 2,3,5-trimethylpyrazine (TMTP), and 2,3,5,6-tetramethylpyrazine (TTMP) are pyrazine compounds with different position substituents (Figure 1(b)). These pyrazines have a pleasant nutty and barbecue flavour that produces a unique aroma [10], which is widely used in the food industry [11–13]. At the same time, these pyrazines are also important flavour substances in liquor, which can be detected in fermented grains by GC-MS [14, 15] (Figure 1(a)). Except for aroma contribution, these pyrazine compounds also play an important role in the pharmaceutical industry. 2,5-DMTP is an important intermediate for the synthesis of new drugs such as amoxicillin and can be used to treat various diseases [16]. TTMP and its derivatives can capture superoxide anion and reduce the production of nitrogen oxide in human granulocytes. It is a clinically active ingredient used in the treatment of cardiocerebral vascular disease [17]. Studies have shown that there is an interaction between pyrazine drugs and albumin [18]. Some pyrazine drugs can bind to albumin to form drug-protein binding complexes, thereby changing the distribution of drugs and tissue targeting [19, 20].

However, there is no report on the interaction between pyrazines and HSA. This study investigated the interaction between pyrazine-flavoured compounds containing different substituents and HSA through multispectral analysis, thermodynamic analysis, binding sites, and molecular dynamics simulation and compared them. In addition, the effects of different pyrazines on the physiological activity of HSA were also investigated. Not only it is of great significance for revealing *in vivo* pharmacokinetics, guiding clinical rational drug use, and developing new drugs but it can also provide useful information for the application of pyrazines in food.

2. Materials and Methods

2.1. Materials. HSA (≥96%) was provided by Sigma-Aldrich Company (Shanghai, China). All the pyrazine flavour substances (≥98%, in pure substance form) were purchased from Macklin Biochemical Co., Ltd. (Shanghai, China). Tris-HCl (pH 7.4, $1.0 \, mol \cdot L^{-1}$) was purchased from Solarbio Bioscience & Technology Co., Ltd. (Shanghai, China). Dimethyl sulfoxide (DMSO, 99%) was purchased from Shanghai Aladdin Biochemical Technology Co., Ltd. (Shanghai, China). HSA was dissolved in Tris-HCl ($0.05 \, mol \cdot L^{-1}$, pH = 7.40) buffer to obtain $1.00 \times 10^{-4} \, mol \cdot L^{-1}$ of HSA. 2,3-DMTP and 2,5-DMTP were dissolved in pure water to obtain solutions with concentrations of $1.875 \times 10^{-3} \, mol \cdot L^{-1}$. TMTP and TTMP were dissolved in ethanol and water, respectively, to obtain the solution with concentrations of $1.875 \times 10^{-3} \, mol \cdot L^{-1}$.

2.2. Fluorescent Quenching. A certain volume of 2,3-DMTP, 2,5-DMTP, TMTP, and TTMP ($1.875 \times 10^{-3} \, mol \cdot L^{-1}$) was added to a cuvette containing 2.5 ml HSA ($1.00 \times 10^{-4} \, mol \cdot L^{-1}$). The 2,3-DMTP, 2,5-DMTP, TMTP, and TTMP concentrations were 0, 7.50, 15.00, 22.50, 30.00,

37.50, 45.00, 52.50, 60.00, and 67.50 ($\times 10^{-6} \, mol \cdot L^{-1}$). The excitation (Ex) wavelength was 285 nm, and the emission (Em) wavelength was recorded from 300 to 420 nm. The slit widths of the Ex and Em wavelengths were set at 15 nm. The fluorescence emission spectra of HSA in different reaction systems were measured at 3 different temperatures (291, 301, and 310 K).

2.3. Three-Dimensional Fluorescence Spectrum. $50 \, \mu L$ of 2,3-DMTP, 2,5-DMTP, TMTP, and TTMP was added to a cuvette containing 2.5 ml of HSA. The Ex was 200 nm, and the Em was set from 200 to 500 nm, and scanned 30 times. The three-dimensional fluorescence spectrum was measured at 301 K.

2.4. Circular Dichroism Spectrum. A certain volume of pyrazine ($1.875 \times 10^{-3} \, mol \cdot L^{-1}$) was added to a quartz cell (a quartz cell of 2 mm path length) containing $350 \, \mu L$ of HSA ($2.00 \times 10^{-6} \, mol \cdot L^{-1}$) with an optical path of 2 mm. The 2,3-DMTP, 2,5-DMTP, TMTP, and TTMP concentrations were 0, 0.46, 0.94, and 1.41 ($\times 10^{-4} \, mol \cdot L^{-1}$). The spectra of HSA in different systems in the range of 200–300 nm were collected at 301 K. Each spectrum presented was the average of three consecutive scans at a scan speed of $100 \, nm \cdot min^{-1}$ and a bandwidth of 1 nm.

2.5. Molecular Dynamics Simulation. Molecular dynamics (MD) simulation was performed for the complex using the GROMACS 2022 software and AMBER 19 force field. Initially, the periodic boundary condition was applied and a cubic box was placed around all atoms with a distance of 10 Å. TIP3P water molecules with a density of $0.10 \, g \cdot mL^{-1}$ were used to solvate the system. The simulation temperature and pressure were controlled at 298 K and 1 bar, respectively. The long-range electrostatic interactions were calculated using the particle mesh Ewald method with an 8 Å cutoff. The time step was 2 fs, and simulation snapshots were saved every 25 ps during the MD simulation. The MD simulation of each system was performed for 200 ns. Finally, the analysis of complex RMSD, SASA, R_g, and protein RMSF was obtained from the MD trajectories, and the analysis of binding energy was conducted using gmx_MMPBSA.

2.6. The Effect of Different Pyrazines on the Physiological Activity of HSA. HSA was mixed with different concentrations of pyrazines for 30 min, and pNPA was added to measure the absorbance of the reaction product at 400 nm. At the same time, the esterase activity of pure HSA was determined under the same conditions [21, 22]. The effects of different pyrazines on HSA esterase activity were obtained. Ellman's reagent was used instead of pNPA to determine the absorbance of the reaction product at 412 nm. The free radical scavenging ability of pure HSA was determined under the same conditions, and the effects of different pyrazine compounds on the free radical scavenging ability of HSA were obtained.
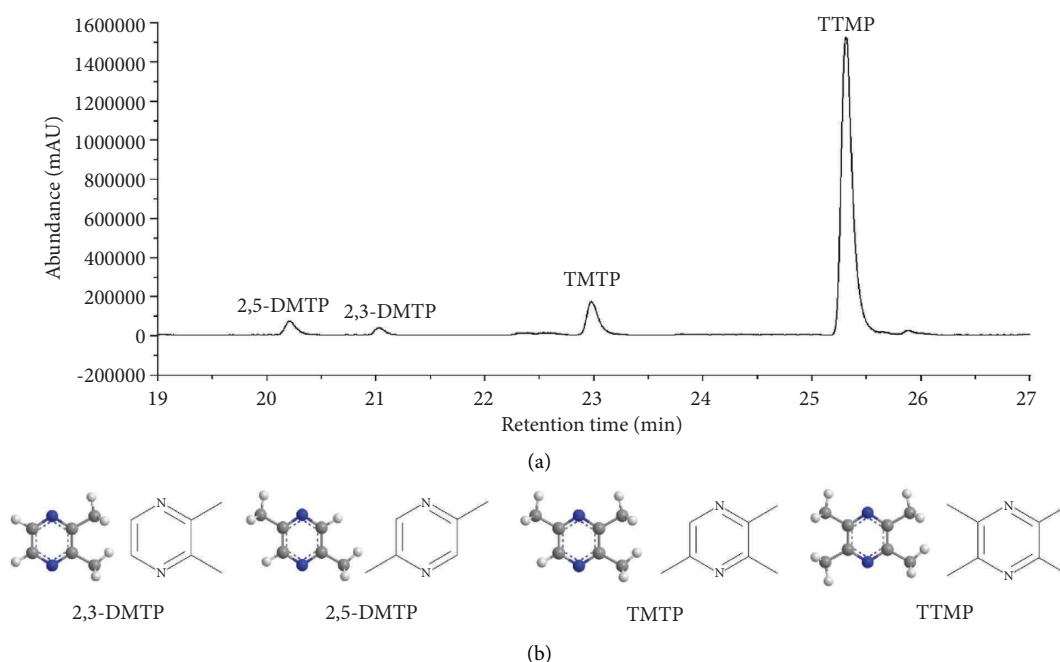
Figure 1: (a) GC-MS plots of pyrazine with different substituents in fermented grains. (b) 2D and 3D structures of different pyrazines.

2.7. Data Processing. The internal filter effect is an important reason for reducing fluorescence intensity. When the absorbance is less than 0.3, the internal filter effect is corrected by the following formula:

$$F_{cor} = F_{obs} \times e^{\frac{A_{ex} + A_{em}}{2}}, \tag{1}$$

where F_{cor} and F_{obs} are the corrected and observed fluorescence intensities, respectively, and A_{ex} and A_{em} are the absorption of the system at the Ex and Em wavelengths, respectively.

3. Results and Discussion

3.1. The Fluorescence Quenching and Quenching Mechanism. Fluorescence quenching refers to the decrease in fluorescence intensity caused by the interaction between fluorescent material molecules and solvent molecules [23]. Figure 2 shows the fluorescence quenching spectra of various pyrazines on HSA at 301 K. With the increase of pyrazine, the fluorescence peak shape of HSA did not change significantly, but the fluorescence intensity decreased gradually. After interaction with four pyrazines, the maximum absorption wavelength of HSA showed different degrees of blueshift. The results showed that 2,3-DMTP, 2,5-DMTP, TMTP, and TTMP could interact with HSA and induce its fluorescence quenching [24]. Fluorescence quenching can be divided into static quenching and dynamic quenching [25]. The fluorescence quenching process is analyzed by the Stern–Volmer equation (2) [26] as follows:

$$\frac{F_0}{F} = 1 + K_{sv}[Q] = 1 + K_q \tau_0 [Q], \tag{2}$$

where F_0 and F are the fluorescence intensities of HSA without quencher and with quencher, respectively, K_{sv} is the dynamic quenching constant, $[Q]$ is the concentration of the quencher, K_q is the bimolecular quenching rate constant, and τ_0 is the average life of HSA without quencher (a value of 10^{-8} s for HSA).

The Stern–Volmer plots for HSA fluorescence quenching by different concentrations of 2,3-DMTP, 2,5-DMTP, TMTP, and TTMP are displayed in Figure 3. The values of K_{sv} and K_q could be obtained from the slopes of a linear adjustment, and the results are summarised in Table 1. The K_{sv} value decreases with the increase in temperature. Meanwhile, the K_q values after the interaction of pyrazines and HSA were greater than the maximum scatter collision quenching constant (2.00×10^{10} L·mol^{-1}·s^{-1}), which indicated that fluorescence quenching of HSA is caused by static quenching [27]. In addition, at the same temperature, the interaction between TTMP and HSA is the strongest.

3.2. UV-Vis Absorption Spectrum. The UV-visible absorption spectrum is caused by the transition of valence electrons after molecules/ions absorb the ultraviolet light or visible light [28]. In the protein molecule, the benzene ring of Tyr, Phe, and Trp residues contains conjugated double bonds, which makes the protein have ultraviolet absorption at 280 nm [29]. The exact mechanism of the quenching process of different pyrazines and HSA was further revealed by the UV-vis absorption spectra (Figure 4). Upon the addition of pyrazines, there were distinct changes in the absorption intensity and peak position of HSA, and the maximum absorption wavelength was blue-shifted. It is indicated that pyrazine compounds can change the conformation of HSA
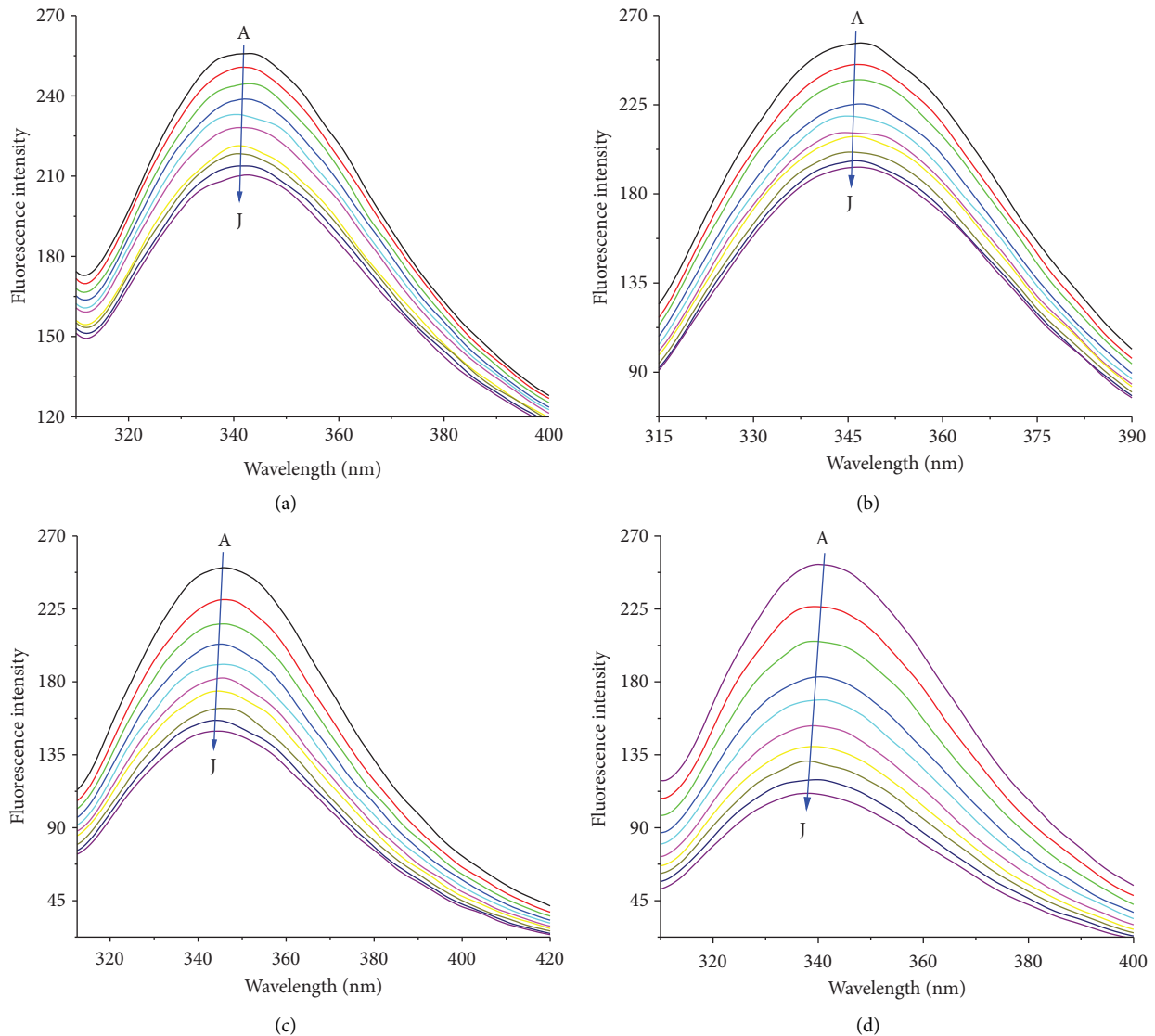
FIGURE 2: Fluorescence quenching spectra of different pyrazines and HSA: (a) 2,3-DMTP, (b) 2,5-DMTP, (c) TMTP, and (d) TTMP. $C_{HSA} = 1.0 \times 10^{-4}$ mol·L^{-1}, $T = 301$ K, and $C_{2,3\text{-DMTP},2,5\text{-DMTP},\text{TMTP},\text{TTMP}}$ (A–J): 0, 7.5, 15, 22.5, 30, 37.5, 45, 52.5, 60, 67.5 ($\times 10^{-6}$ mol·L^{-1}).

and increase the hydrophobicity of aromatic amino acid hydrophobic groups in HSA molecules [30]. Since the dynamic quenching only affects the excited fluorescent molecules, it does not change the absorption intensity of the absorption spectrum. However, static quenching can interact with fluorescent molecules to form complexes, causing changes in the absorption intensity of fluorescent molecules [31]. Therefore, the quenching process of different pyrazines and HSA is static quenching.

3.3. Combining Properties and Thermodynamic Parameters. The binding constant (K_a) is a parameter for quantifying the interaction between small molecules and proteins. The binding site (n) refers to the specific site in the molecule that can form a stable interaction with the ligand. The K_a and n can be calculated by equation (3) [32].

There are four fundamental forces that affect the interaction between proteins and ligands, namely, hydrogen bond, electrostatic force, hydrophobic interaction, and van der Waals force, which can be evaluated by thermodynamic parameters. The thermodynamic parameters were calculated by Van't Hoff equations (4)–(6) [33].

$$\log \frac{(F_0 - F)}{F} = \log K_a + n \log [Q], \tag{3}$$

$$\ln K_a = -\frac{\Delta H}{RT} + \frac{\Delta S}{R}, \tag{4}$$

$$\Delta G = -RT \ln K_a, \tag{5}$$

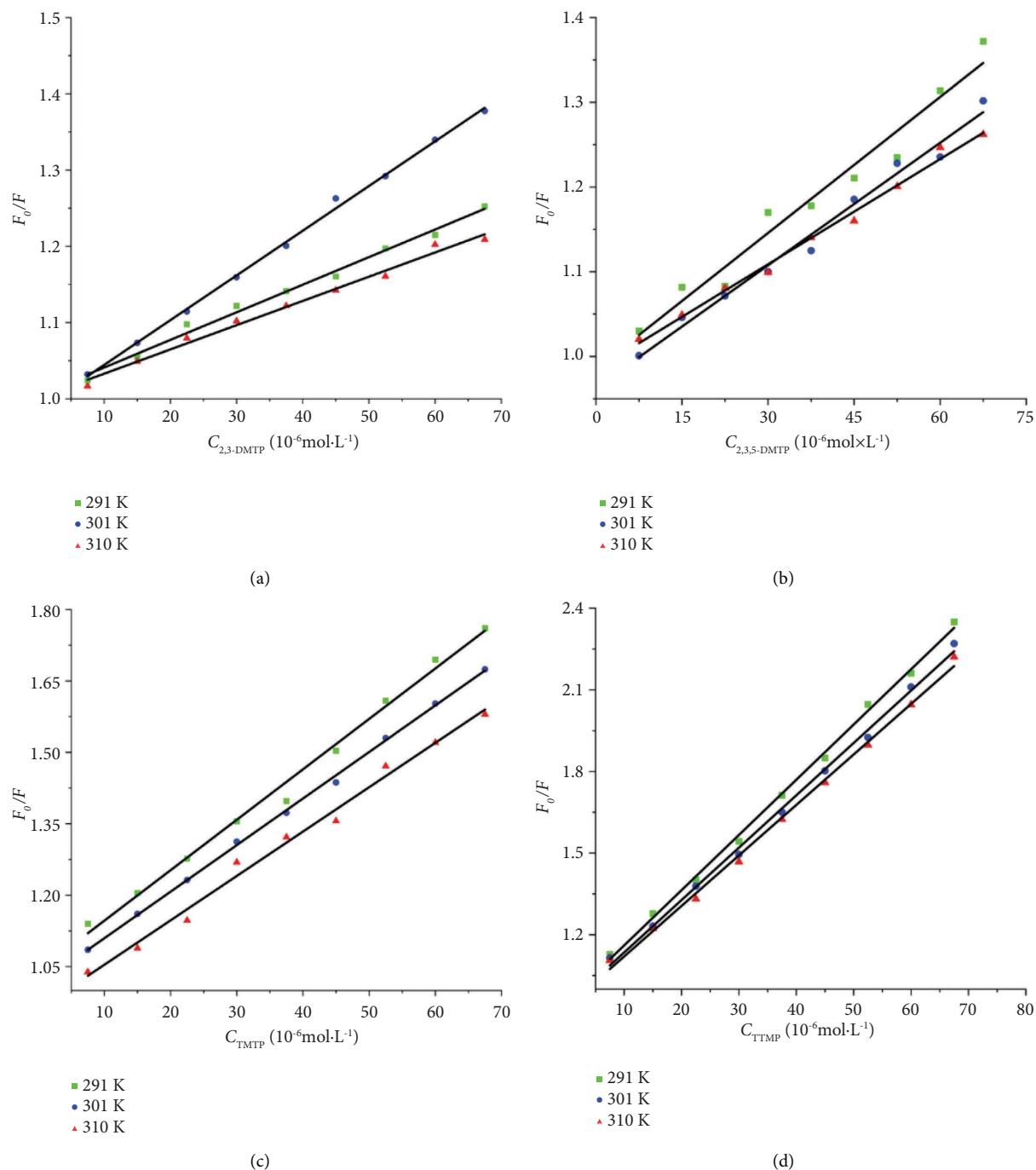$$\Delta S = \frac{\Delta H - \Delta G}{T}, \tag{6}$$

Figure 3: Stern–Volmer diagrams of fluorescence quenching of HSA at three different temperatures: (a) 2,3-DMTP, (b) 2,5-DMTP, (c) TMTP, and (d) TTMP.

where K_a is the binding constant that reflects the strength of the interaction of proteins acting with small molecules at the corresponding temperatures, n is the number of binding sites, $[Q]$ is the concentration of FA or FAM, T is the temperature, and R is the gas constant. ΔH, ΔS, and ΔG are the enthalpy change, entropy change, and Gibbs free energy, respectively.

Figure 5 shows the double logarithmic curve of the interaction between pyrazine compounds and HSA. Based on the slope and constant, the binding site and the binding constant

can be calculated (Table 2). K_a increases with the temperature, indicating that the binding ability of pyrazine compounds to HSA is strong. At the same temperature, the binding force of pyrazine compounds with HSA can be described as follows: TMTP < 2,5-DMTP < 2,3-DMTP < TTMP. This result indicated that the more substituents, the easier it is to bind to HSA. The position of the substituent also affects the binding effect with HSA. Compared with the parasubstituent, the orthosubstituent is easier to bind to HSA. In addition, n is close to 1, and there is only one binding site between HSA and

TABLE 1: Quenching constants of HSA at different temperatures.

|	T (K)	K_{sv} (L·mol^{-1})	K_q (L·mol^{-1}·s^{-1})	R
2,3-DMTP	291	6.332×10^3	6.332×10^{11}	0.9920
	301	5.865×10^3	5.865×10^{11}	0.9979
	310	5.656×10^3	5.656×10^{11}	0.9905
2,5-DMTP	291	5.315×10^3	5.315×10^{11}	0.9662
	301	4.820×10^3	4.820×10^{11}	0.9853
	310	4.139×10^3	4.139×10^{11}	0.9924
TMTP	291	1.059×10^4	1.059×10^{12}	0.9928
	301	9.778×10^3	9.778×10^{11}	0.9989
	310	9.319×10^3	9.319×10^{11}	0.9903
TTMP	291	2.029×10^4	2.029×10^{12}	0.9978
	301	1.924×10^4	1.924×10^{12}	0.9973
	310	1.855×10^4	1.855×10^{12}	0.9970
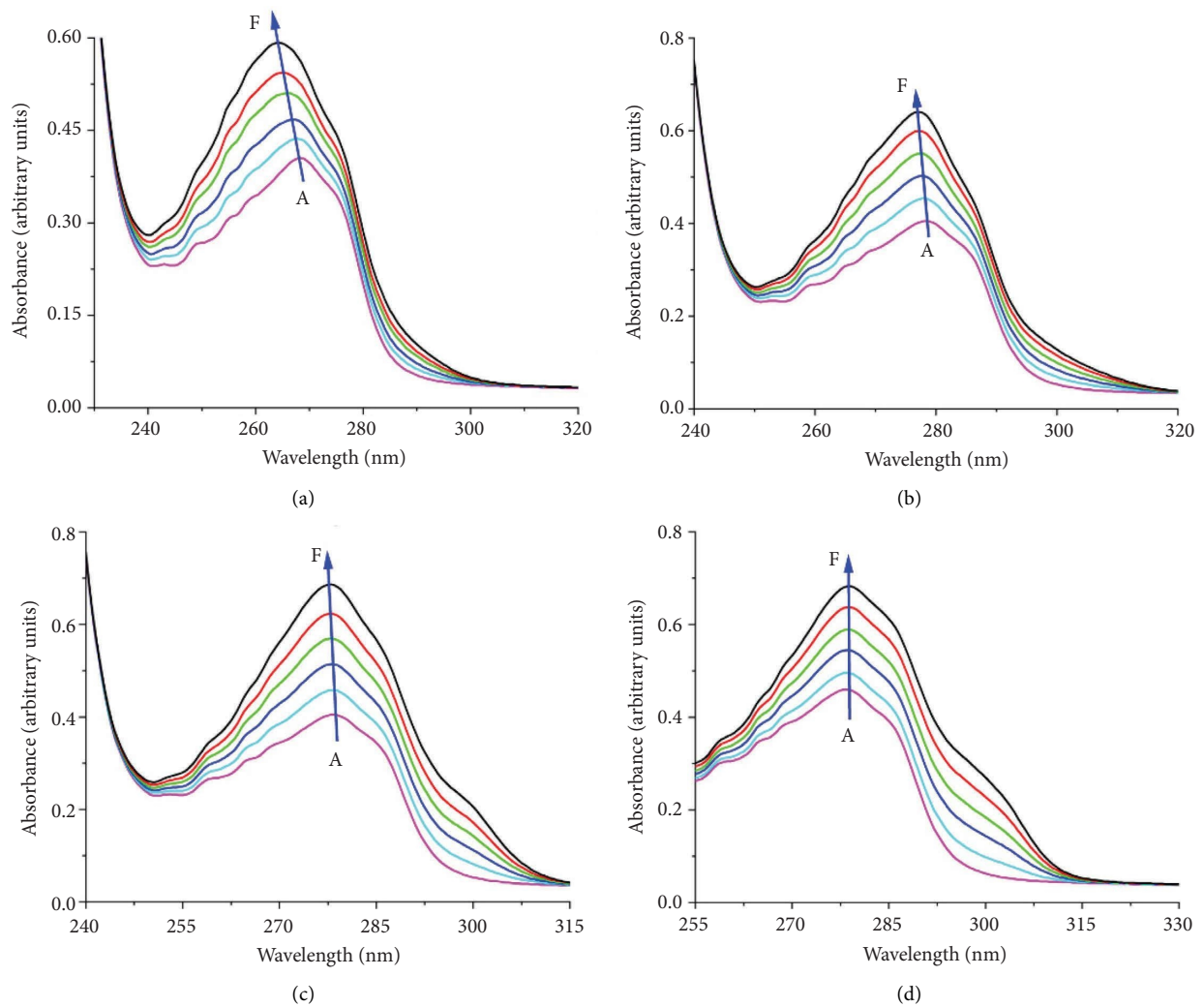
FIGURE 4: UV-vis absorption spectra of HSA in the presence of different pyrazines: (a) 2,3-DMTP, (b) 2,5-DMTP, (c) TMTP, and (d) TTMP, $C_{HSA} = 1.25 \times 10^{-5}$ mol·L^{-1}, $T = 301$ K, and $C_{2,3\text{-DMTP},2,5\text{-DMTP,TMTP,TTMP}}$ (A–F): 0, 0.75, 1.5, 2.25, 3.0, 3.75 ($\times 10^{-5}$ mol·L^{-1}).
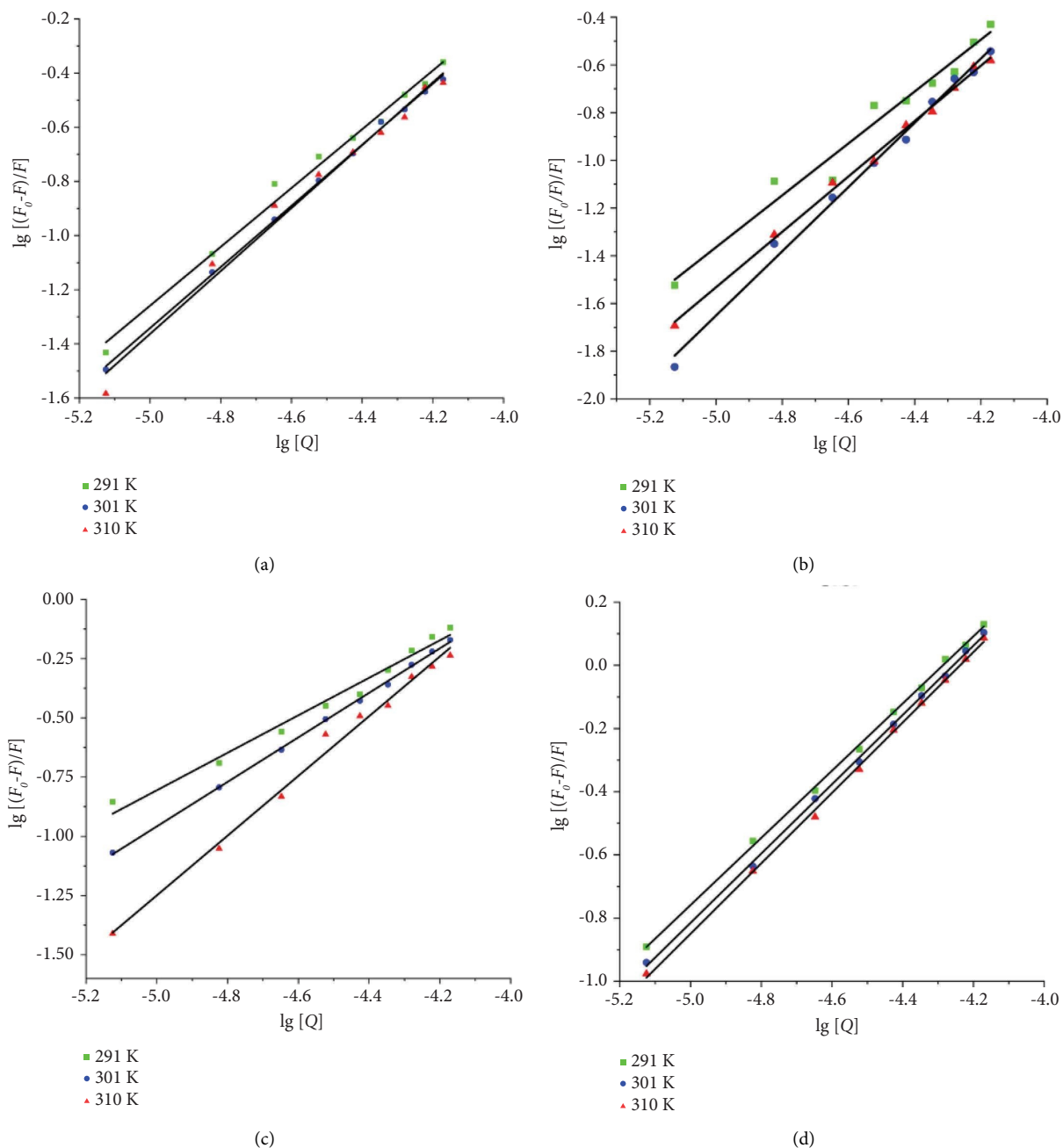
(a)

(b)

(c)

(d)

FIGURE 5: Double logarithmic curves of various systems at different temperatures: (a) 2,3-DMTP, (b) 2,5-DMTP, (c) TMTP, and (d) TTMP.

pyrazine compounds. The thermodynamic parameters are shown in Table 2. $\Delta G < 0$, indicating that the reaction can proceed spontaneously. $\Delta H > 0$, $\Delta S > 0$, indicating that hydrophobic force is the main force between pyrazine compounds and HSA [34], which once more proves that pyrazine compounds can interact with HSA.

3.4. Energy Transfer in the Interaction between HSA and Pyrazines. Energy transfer can be used to evaluate the distance between the ligand and Trp residue in the protein [35]. Based on Förster's nonradiative energy transfer theory,

the distance between pyrazines and HSA luminescent groups can be calculated by using the following equations [36, 37]:

$$E = 1 - \frac{F}{F_0} = \frac{R_0^{\,6}}{R_0^{\,6} + r^6}, \tag{7}$$

$$R_0^{\,6} = 8.8 \times 10^{-25} K^2 \varnothing N^{-4} J, \tag{8}$$

$$J = \frac{\sum F(\lambda)\varepsilon(\lambda)\lambda^4 \Delta\lambda}{\sum F(\lambda)\Delta\lambda}, \tag{9}$$

TABLE 2: Binding constants, number of binding sites, and thermodynamic parameters of 2,3-DMTP, 2,5-DMTP, TMTP, and TTMP interacting with HSA at different temperatures.

	T (K)	K_a (L·mol^{-1})	n	R	ΔH (kJ·mol^{-1})	ΔG (L·mol^{-1})	ΔS (L·mol^{-1})
2,3-DMTP	291	1.4696×10^4	1.0852	0.9908		-23.26	
	301	1.9888×10^4	1.1281	0.9987	24.84	-24.77	165.04
	310	2.7631×10^4	1.1609	0.9843		-26.36	
2,5-DMTP	291	1.1956×10^4	1.0884	0.9705		-22.72	
	301	1.2930×10^4	1.1056	0.9916	17.62	-23.70	138.17
	310	1.8858×10^4	1.1615	0.9968		-25.37	
TMTP	291	1.4083×10^3	0.7909	0.9813		-17.54	
	301	5.4731×10^3	0.9393	0.9991	170.66	-21.54	644.16
	310	1.1243×10^4	1.2600	0.9915		-29.98	
TTMP	291	3.6091×10^4	1.0632	0.9990		-25.39	
	301	4.6655×10^4	1.0968	0.9991	15.17	-26.90	139.50
	310	5.2856×10^4	1.1145	0.9989		-28.03	

where K^2 is the dipole spatial orientation factor, N is the refractive index of the medium, Φ is the fluorescence quantum yield of the donor in the presence of no acceptor, $F(\lambda)$ is the fluorescence intensity of the donor at wavelength λ, and $\varepsilon(\lambda)$ is the molar absorption of the acceptor at wavelength λ. Among them, $K^2 = 2/3$, $N = 1.336$, and $\Phi = 0.118$.

When the concentration of pyrazines and HSA is 1 : 1, the overlap of HSA fluorescence spectra and different pyrazine absorption spectra is shown in Figure 6. The relationship between energy overlap integral (J), energy transfer efficiency (E), critical distance (R_0), and binding distance (r) is shown in Table 3. The binding distances of 2,3-DMTP, 2,5-DMTP, TTMP, and TMTP with HSA were calculated to be 2.99 nm, 2.82 nm, 3.49 nm, and 4.22 nm, respectively. $r < 7$ nm and $0.5R_0 < r < 1.5R_0$ indicate that the chromophore in HSA can transfer energy to pyrazine compounds by nonradiation. $r > R_0$ of the interaction between 2,3-DMTP, 2,5-DMTP, TMTP, and HSA indicated that the contribution of nonradiative energy transfer to fluorescence quenching was small in these three systems. In summary, the endogenous fluorescence quenching mechanism of pyrazine compounds on HSA is mainly static quenching, which is consistent with the conclusion of the fluorescence quenching mechanism [38].

3.5. Synchronous Fluorescence Spectrum. Synchronous fluorescence measurement can provide microenvironment information on molecules near fluorophore functional groups [39]. When $\Delta\lambda = 15$ nm and 50 nm, the synchronous fluorescence reflects the fluorescence characteristics of Tyr and Trp residues, respectively. As shown in Figure 7, the fluorescence intensity of HSA decreased with the increase in pyrazine concentration, that is, the change in amino acid environment and hydrophobicity of HSA. At $\Delta\lambda = 15$ nm, the maximum emission wavelength of HSA in the TMTP-HSA, 2,3-DMTP-HSA, 2,5-DMTP-HSA, and TTMP-HSA systems showed a significant redshift, indicating that 2,3-DMTP, 2,5-DMTP, TMTP, and TTMP increase the polarity around Tyr residues in HSA [40, 41]. At $\Delta\lambda = 50$ nm, the maximum emission wavelength of HSA in the 2,3-DMTP-HSA and 2,5-DMTP-HSA systems showed

a significant redshift, and there is no significant change in the maximum emission wavelength of HSA interacting with TTMP and TMTP, indicating that 2,3-DMTP and 2,5-DMTP increase the polarity around Tyr residues in HSA. In summary, pyrazine compounds can enhance the polarity of the microenvironment around amino acid residues in HSA, change the secondary structure of HSA protein, and lead to changes in the conformation of HSA. Moreover, the redshift of HSA was more significant when $\Delta\lambda = 15$ nm, indicating that the fluorescence quenching intensity of pyrazine compounds to Tyr was greater than that to Trp.

3.6. Circular Dichroism (CD). In order to further explore the effect of pyrazine compounds on the conformation of HSA, the circular dichroism (CD) of different pyrazine compounds on HSA was determined. As shown in Figure 8, two negative peaks appear in the spectrum, and it is the characteristic peak of the α-helix structure in HSA [42]. The intensity of the two peaks gradually decreases as the concentration of pyrazines in the HSA solution increases. The SELCON3 algorithm was used to calculate the proportion of different types of secondary structures in HSA molecules with the addition of pyrazine compounds. The results are shown in Table 4. With the addition of pyrazines, the α-helix structure in HSA molecules decreased, while the content of β-Sheet, β-Turn, and random coil structure in protein molecules increased. The change of secondary structure indicated that pyrazine compounds changed the microenvironment around HSA and changed the secondary structure of HSA. At the same time, this further indicates that the interaction between pyrazine and amino acid residues on the peptide chain of HSA destroys the network structure of hydrogen bonds and loosens the conformation of HSA.

3.7. Three-Dimensional Fluorescence Spectrum. The three-dimensional fluorescence spectroscopy can simultaneously obtain fluorescence intensity information from two different dimensions of excitation and emission, and the changes in HSA structure can be observed more comprehensively and intuitively [43]. Figure 9 shows the three-dimensional fluorescence spectrum of 2,3-DMTP, 2,5-DMTP, TMTP,
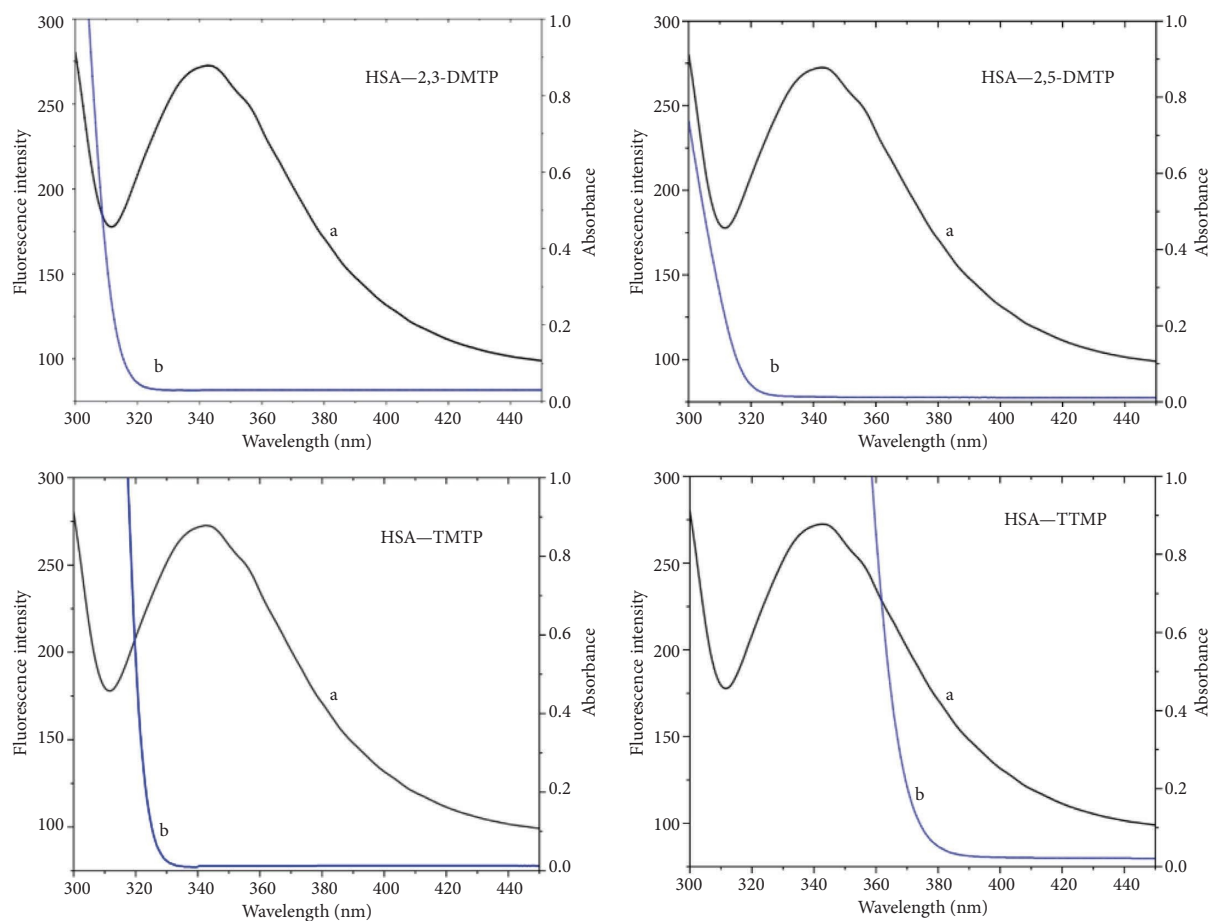
FIGURE 6: The fluorescence spectrum (a) of HSA overlaps the absorption spectrum (b) of pyrazines. $C_{HSA} = C_{2,3\text{-}DMTP,2,5\text{-}DMTP,TMTP,TTMP} = 1.00 \times 10^{-5}$ mol·L^{-1} and $T = 301$ K.

TABLE 3: Parameters related to the energy transfer process between HSA and pyrazines.

	J (cm^3·mol^{-1}·L^{-1})	E	R_0 (nm)	r (nm)
2,3-DMTP	1.85×10^{-14}	0.2740	2.54	2.99
2,5-DMTP	1.14×10^{-14}	0.2447	2.34	2.82
TMTP	8.40×10^{-14}	0.4027	3.27	3.49
TTMP	49.30×10^{-14}	0.5594	4.39	4.22

and TTMP interacting with HSA. Among them, peak 1 and peak 2 are Rayleigh scattering peaks. The peak a is the fluorescence peak of Trp and Tyr residues, which mainly reflects the changes in Trp and Tyr spectra caused by $n \longrightarrow \pi^*$ transitions. The peak b is the characteristic peak of the peptide backbone, which reflects the spectral changes of the HSA peptide backbone caused by $\pi \longrightarrow \pi^*$ transitions [44]. It can be seen from the figure that the addition of pyrazine significantly reduced the fluorescence intensity of peak a and peak b. At the same time, the emission wavelength corresponding to the maximum absorption peak of peak b shifted significantly. It is fully demonstrated that pyrazine compounds lead to changes in the spatial conformation of HSA, which changes the internal microenvironment of the molecule and reduces the luminous efficiency of Trp and Tyr residues.

3.8. Resonance Light Scattering (RLS). When the excitation light is located in or close to the molecular absorption band, the electron strongly absorbs the light energy due to resonance, resulting in resonance light [45]. RLS is very sensitive to electrostatic interactions, hydrogen bonding, and hydrophobic interactions [46], which can be used to characterize changes in the concentration and aggregation state of the species. With the addition of pyrazine compounds, the RLS intensity of HSA showed a downward trend (Figure 10). After the combination of pyrazine compounds with HSA, the protective water layer on the surface of HSA was destroyed, which made the originally more dispersed protein become more dispersed, and the protein size in HSA decreased along with the degree of aggregation.

3.9. Molecular Docking. Molecular docking is the process of identifying two or more molecules by geometric matching and energy matching to find the best matching mode, which is helpful in further understanding the interaction between molecules [47]. The docking energy (Table 5) and interaction (Figure 11) of different substituent pyrazines binding to HSA can be obtained by molecular docking. The docking energy represents the binding capacity of each pyrazine compound and HSA, and the lower the docking energy, the
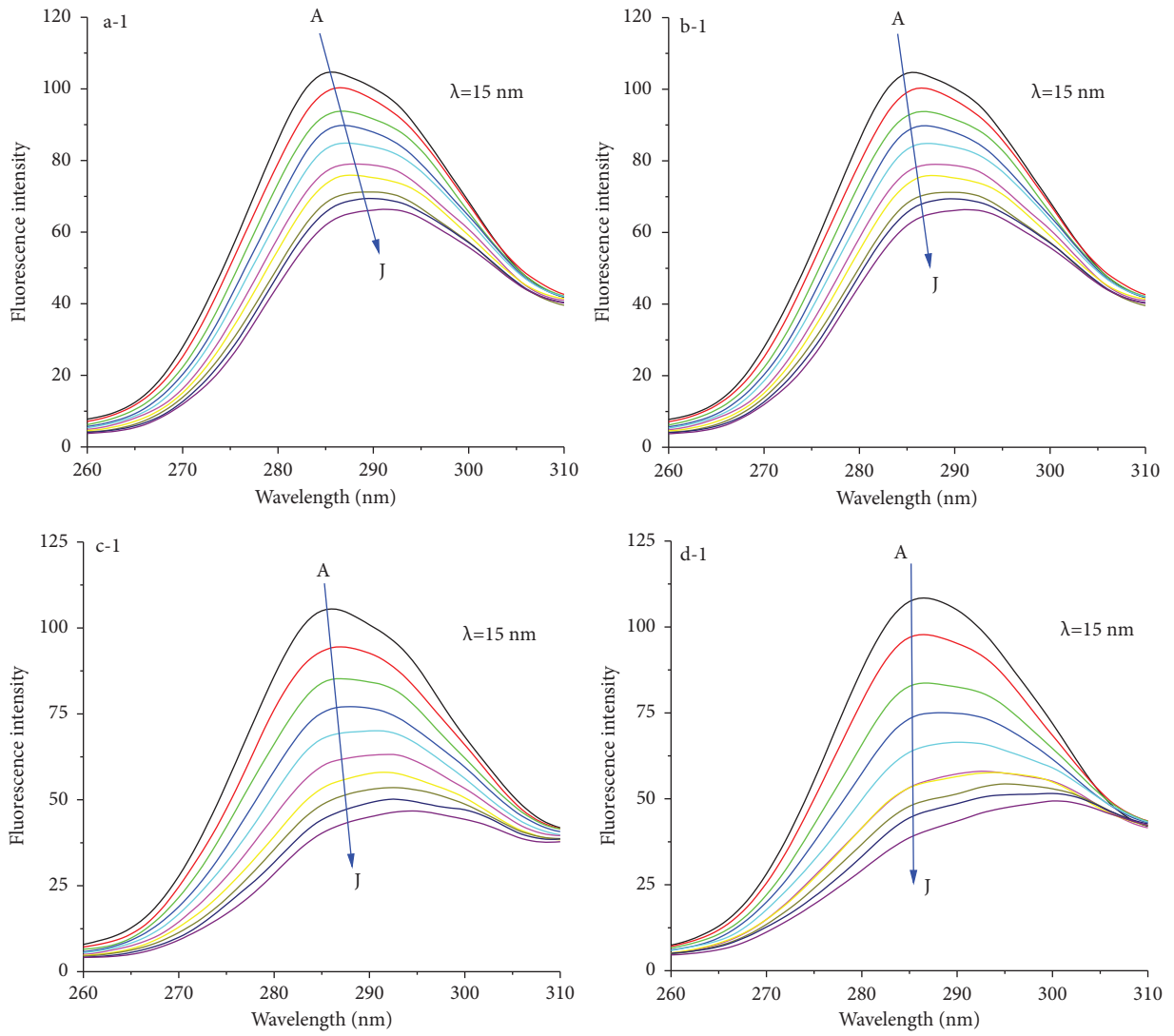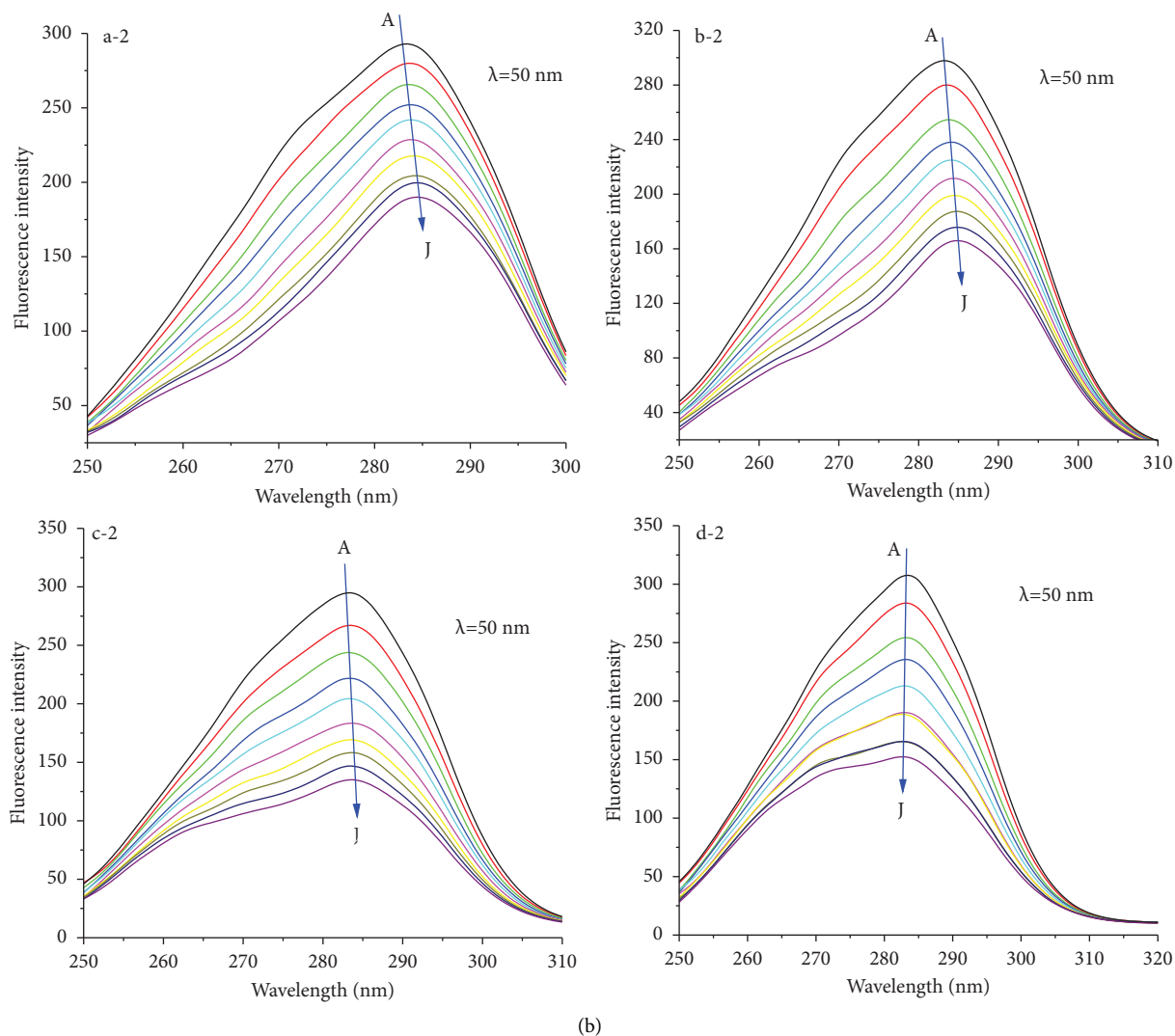
(a)

FIGURE 7: Continued.

Figure 7: Synchronous fluorescence spectra of different pyrazines and HSA: (a) 2,3-DMTP, (b) 2,5-DMTP, (c) TMTP, and (d) TTMP. $C_{HSA} = 1.00 \times 10^{-4}$ mol·L^{-1}, $T = 301$ K, and $C_{2,3-DMTP,2,5-DMTP,TMTP,TTMP}$ (A–J): 0.0, 7.5, 15, 22.5, 30, 37.5, 45, 52.5, 60, 67.5 ($\times 10^{-6}$ mol·L^{-1}).
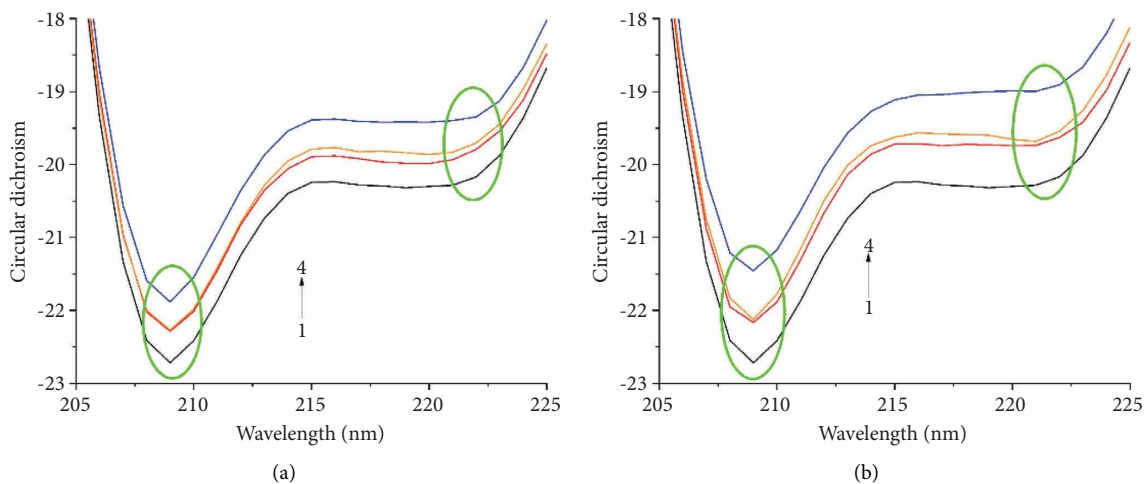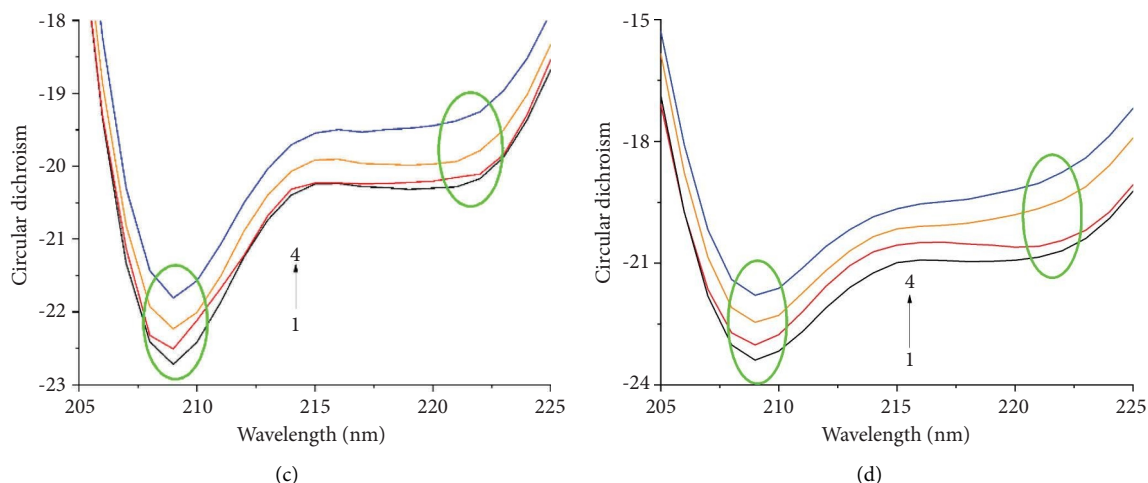

Figure 8: Continued.

(c)

(d)

FIGURE 8: Circular dichroism of the interaction between different substituents of pyrazine and HSA: (a) 2,3-DMTP, (b) 2,5-DMTP, (c) TMTP, and (d) TTMP. $C_{HSA} = 2.0 \times 10^{-6}$ mol·L^{-1} and $C_{2,3-DMTP,2,5-DMTP,TMTP,TTMP}$ (1–4) = 0, 0.46, 0.94, 1.41 ($\times 10^{-4}$ mol·L^{-1}).

TABLE 4: Conformational changes of HSA with different substituent pyrazine compounds.

	α-Helix (%)	β-Sheet (%)	β-Turn (%)	Random coil (%)
	61.7	7.5	12.9	17.6
2,3-DMTP	60.4	7.9	13	18.2
	58.9	8.2	13.2	18.8
	57.2	8.6	13.4	19.6
	61.7	7.5	12.9	17.6
2,5-DMTP	59.9	7.9	13.1	18.4
	57.7	8.5	13.4	19.4
	56	8.9	13.6	20.2
	61.7	7.5	12.9	17.6
TMTP	60.3	7.9	13.1	18.2
	59.1	8.1	13.2	18.8
	58.9	8.2	13.2	18.9
	62.4	7.4	12.8	17.3
TTMP	61.6	7.6	12.9	17.6
	60.1	7.9	13.1	18.3
	58.1	8.4	13.3	19.2

more stable the binding between the ligand and the receptor [48]. It is generally believed that the docking energy value less than −4.25 kcal/mol^{-1} indicates that there is a certain binding activity between the two, less than −5.0 kcal/mol^{-1} indicates a good binding activity, and less than −7.0 kcal/mol^{-1} indicates a strong binding activity [49]. It can be seen from the table that the binding energy of different substituent pyrazine compounds and HSA is between −7.0 kcal·mol^{-1} and −5.0 kcal·mol^{-1}, and the binding activity of pyrazines to HSA is TTMP > TMTP > 2,3-DMTP > 2,5-DMTP. This also proves that the more the substituents of pyrazine compounds, the easier it is to bind to HSA. Compared with the parasubstituent, the orthosubstituent is easier to bind to HSA.

During the interaction, four pyrazines formed hydrophobic interactions with Ala158, Tyr138, Ile142, Tyr161, and Phe165 residues in HSA (Figure 11). In addition, 2,3-DMTP, TMTP, and TTMP also formed hydrophobic interactions with Phe134 residues (Figures 11(a), 11(c), and 11(d)). TMTP formed a hydrophobic interaction with Met123 (Figure 11(c)). It can be seen from the above that 2,3-DMTP, 2,5-DMTP, TMTP, TTMP, and HSA are mainly combined by hydrophobic force. This further verifies the thermodynamic results. In the part of three-dimensional fluorescence spectroscopy, we found that the fluorescence peak of Trp and Tyr residues decreased significantly. Furthermore, molecular docking proved that the contribution of Tyr was greater than that of Trp in the interaction with pyrazine compounds.

3.10. Molecular Dynamics (MD) Simulation. The trend of root-mean-square displacement (RMSD) of proteins and ligands is an important characterization to determine whether the simulation is stable [50]. The height of RMSD reflects the overall deviation of the trajectory from the reference molecule [51]. The RMSD calculation results are shown in Figure 12(a). The overall structure of the complex was balanced in an MD simulation time of 200 ns. The RMSD of free HSA fluctuates more than the complex. At the same time, HSA after binding to different pyrazines is more stable than protein (Figure 12(a-1)). It is shown that pyrazines made the structure of HSA more stable. In addition, the RMSD values of HSA and TTMP complexes were lower and fluctuated less than those of other pyrazines and HSA complexes, indicating that TTMP and HSA bound stronger. TMTP binds weakest to HSA, and 2,5-DMTP and 2,3-DMTP are not much different. These are consistent with the previous analysis of the associative constant.

To gain insight into the conformational changes of HSA, root-mean-square fluctuations (RMSFs) were used to measure the intensity of change in the secondary structure of HSA [52]. Compared with the RMSF of different complexes after pyrazines binding to HSA, the RMSF fluctuations simulated by free HSA molecular dynamics were greater (Figure 12(b)), indicating that HSA was more stable after
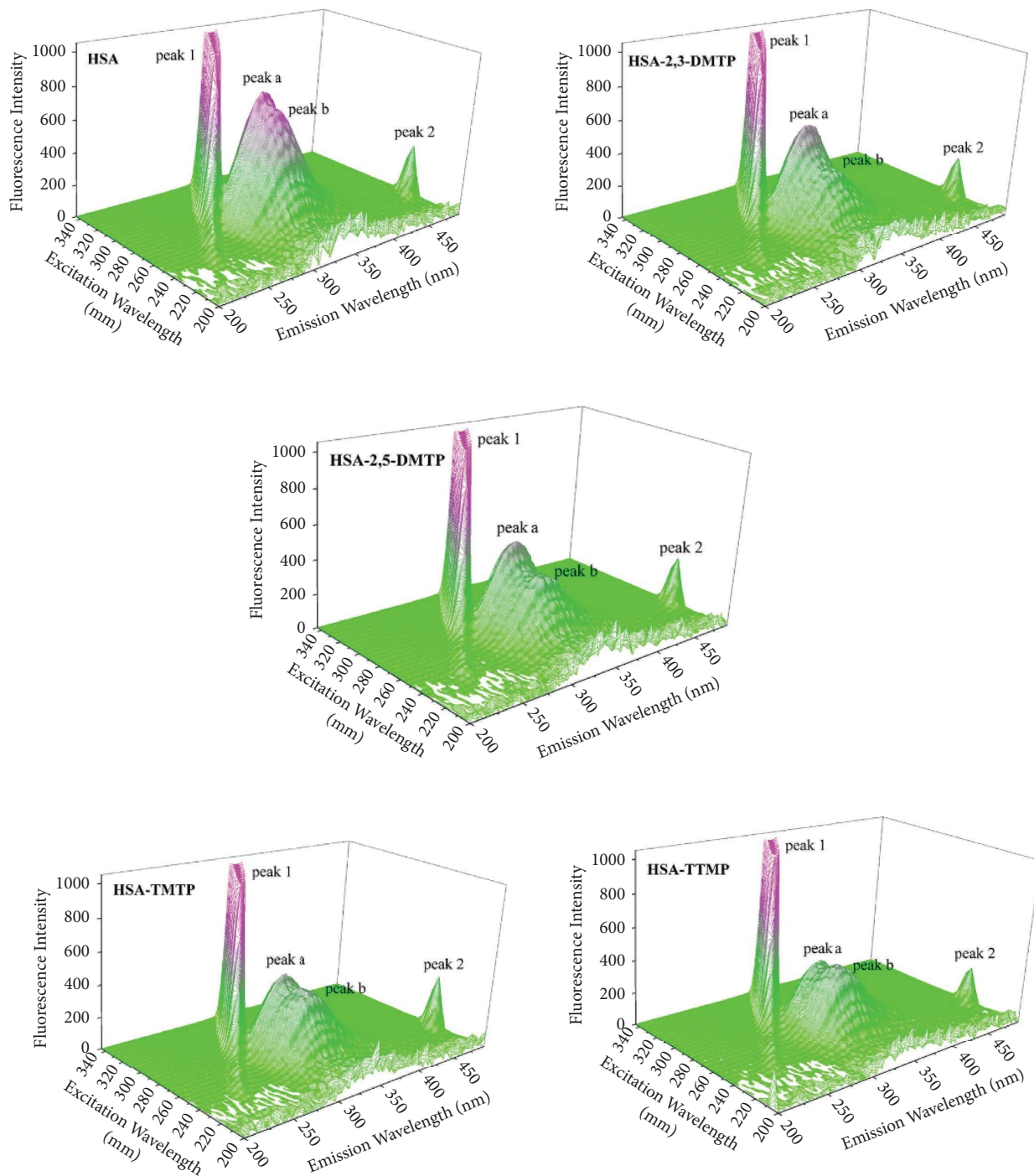
FIGURE 9: Three-dimensional fluorescence spectra of different pyrazine interactions with HSA.

binding to pyrazines. At the same time, the RMSF value decreased to a certain extent after HSA was combined with different pyrazines. Among them, the RMSF value of the complex was lower than that of other pyrazine compounds after HSA was combined with TTMP, indicating that TTMP greatly increased the stability of HSA. The reason for this result may be related to the number and position of substituents.

The radius of rotation (R_g) is a physical quantity that describes the structural compactness of lactoglobulin, and smaller values indicate greater lactoglobulin density [53]. R_g reacts to the volume and shape of proteins, helping to study protein compactness [54]. R_g simulated by free HSA dynamics was greater than that of the complex, indicating that the complex was more stable and the system was tighter after binding to different pyrazines (Figure 12(c)). Among them,
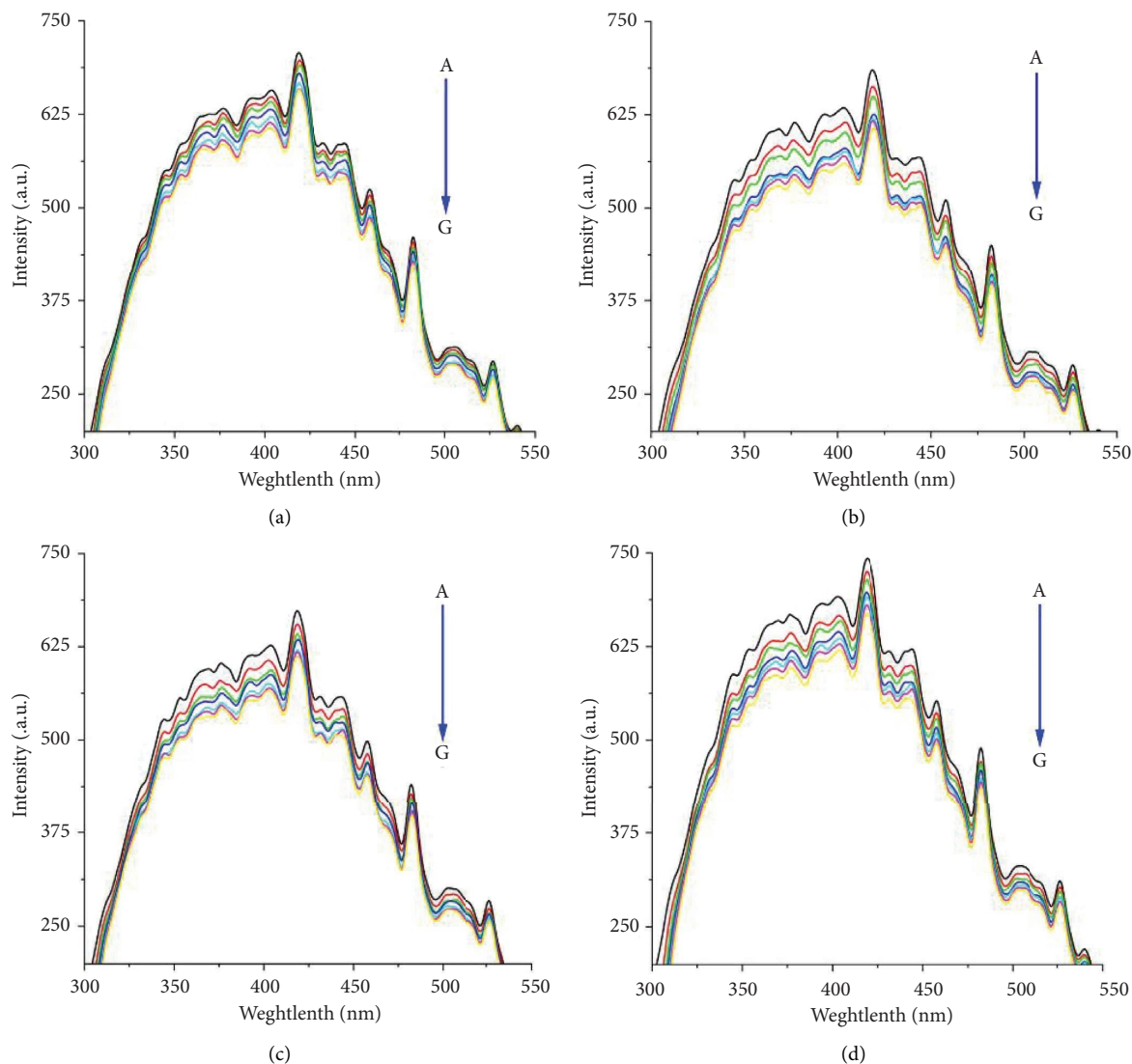
(a)

(b)

(c)

(d)

FIGURE 10: RLS spectra of the interaction between different substituents of pyrazine and HSA. $C_{HSA} = 1.0 \times 10^{-5}$ mol·L^{-1} and C$_{2,3\text{-DMTP, 2,5-DMTP, TMTP, TTMP}}$ (A–G) = 0, 1.5, 3.0, 4.5, 6.0, 7.5, 9.0 ($\times 10^{-5}$ mol·L^{-1}).

TABLE 5: Docking energy of interaction between different pyrazines and HSA.

Small molecule	Bonding energy (kcal·mol^{-1})
2,3-DMTP	−5.1
2,5-DMTP	−5.0
TMTP	−5.7
TTMP	−6.1

TTMP was the most tightly bound to HSA, followed by 2,3-DMTP and 2,5-DMTP, and TMTP was the least tightly bound to HSA. This structure was consistent with RMSD and RMSF analyses.

Solvent-accessible surface area (SASA) is the surface area of biomolecules accessible to solvents [55]. The SASA of the complex was analyzed (Figure 12(d)). After different pyrazines and HSA binding, the SASA of the complex decreased compared with the SASA of free HSA, indicating that the protein structure stability of HSA

increased. At the same time, the conformations before and after MD are superimposed to generate porcupine diagrams to represent the changes in protein structure after small molecule binding (Figure 13) and the arrow indicates the movement direction of the protein amino acid residue, and the length of the arrow represents the size of the travel distance. After small molecules bind to the active site of HSA, HSA has strong movement, indicating that different pyrazines have a greater effect on the structure of HSA.

3.11. The Effect of Different Pyrazines on the Physiological Activity of HSA. HSA has esterase activity, can hydrolyze pNPA to produce p-nitrophenol, and has the maximum absorption at 400 nm [56]. The esterase activity of HSA decreases with the increase of pyrazine concentration (Figure 14(a)). The reason for this result is that the addition of pyrazines increases the folding degree of HSA, exposing
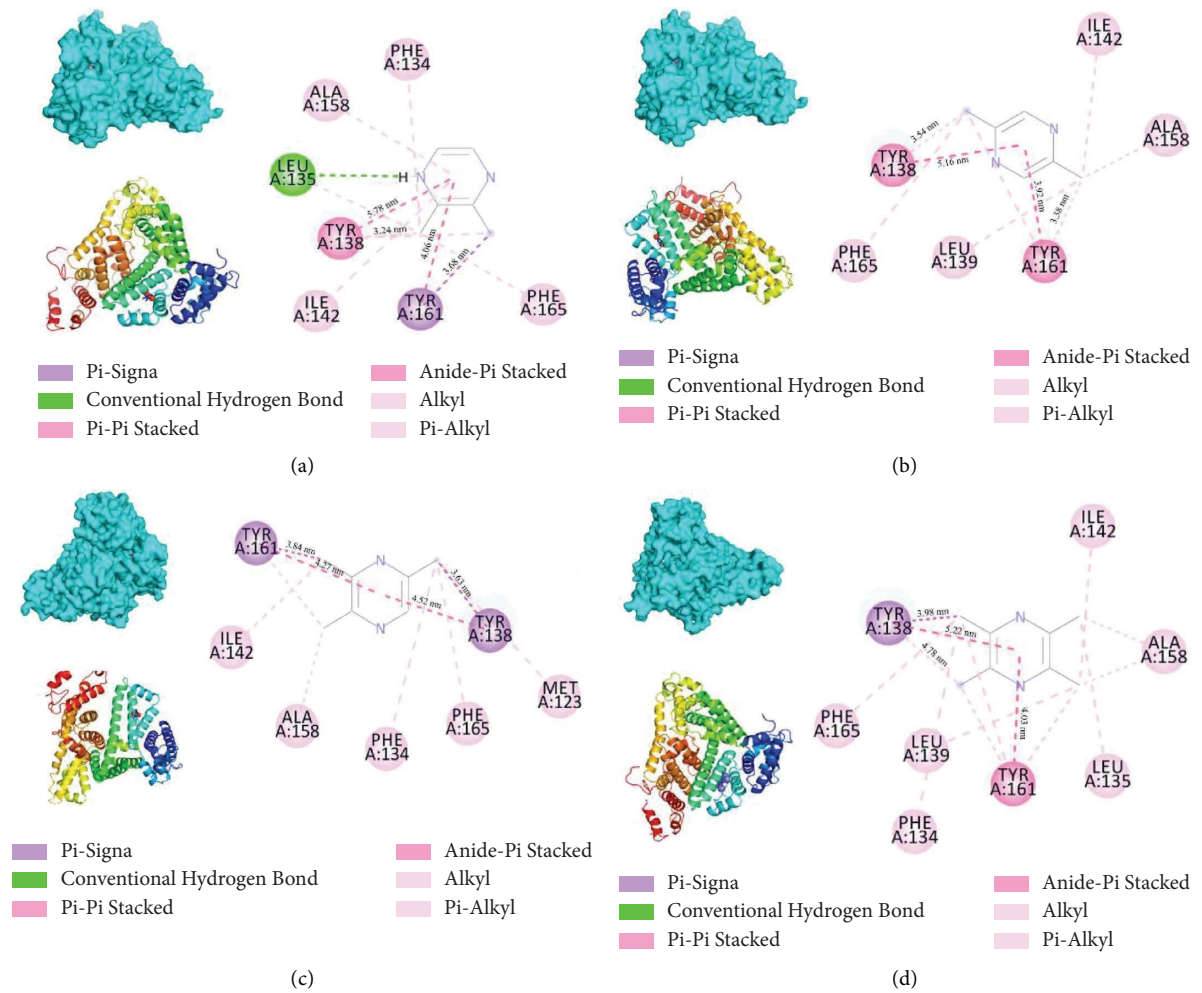
Figure 11: Molecular docking diagram of different pyrazines with HSA: (a) 2,3-DMTP, (b) 2,5-DMTP, (c) TMTP, and (d) TTMP.
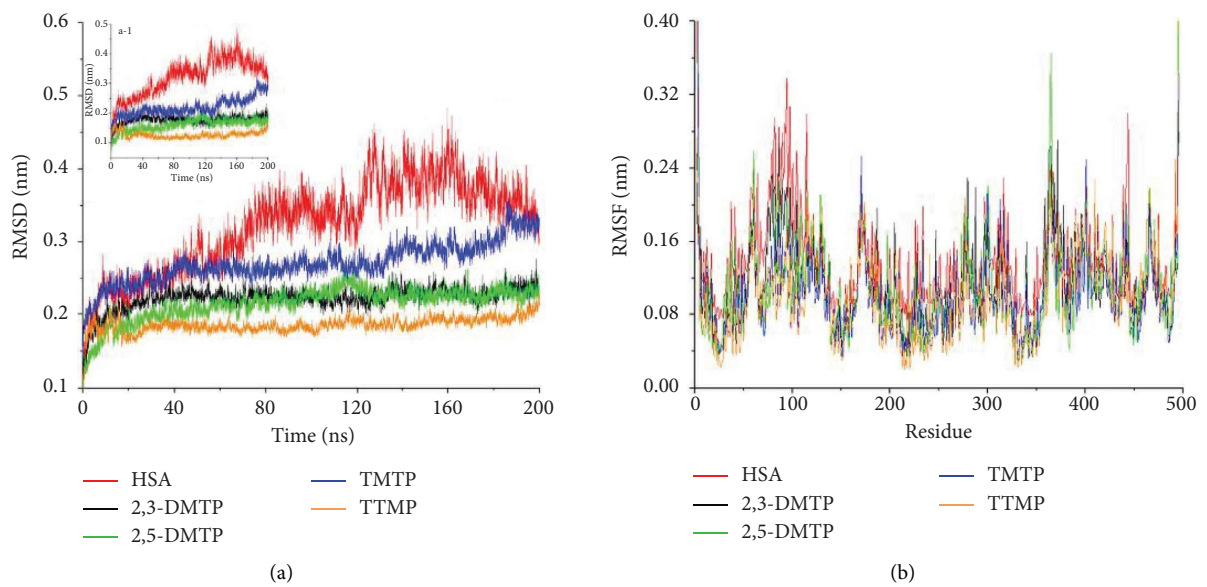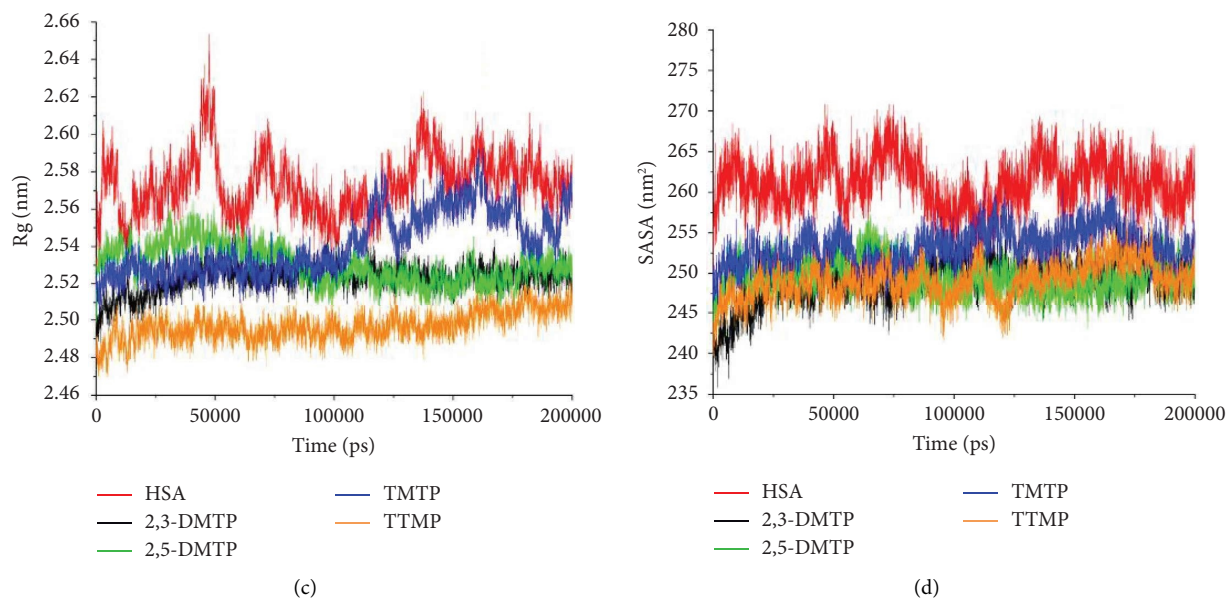

Figure 12: Continued.

FIGURE 12: MD simulation of different pyrazine and HSA interactions: (a) RMSD variation diagram of free HSA and complex, (b) RMSF variation diagram of free HSA and complex, (c) R_g variation diagram of free HSA and complex, and (d) SASA variation diagram of free HSA and complex.
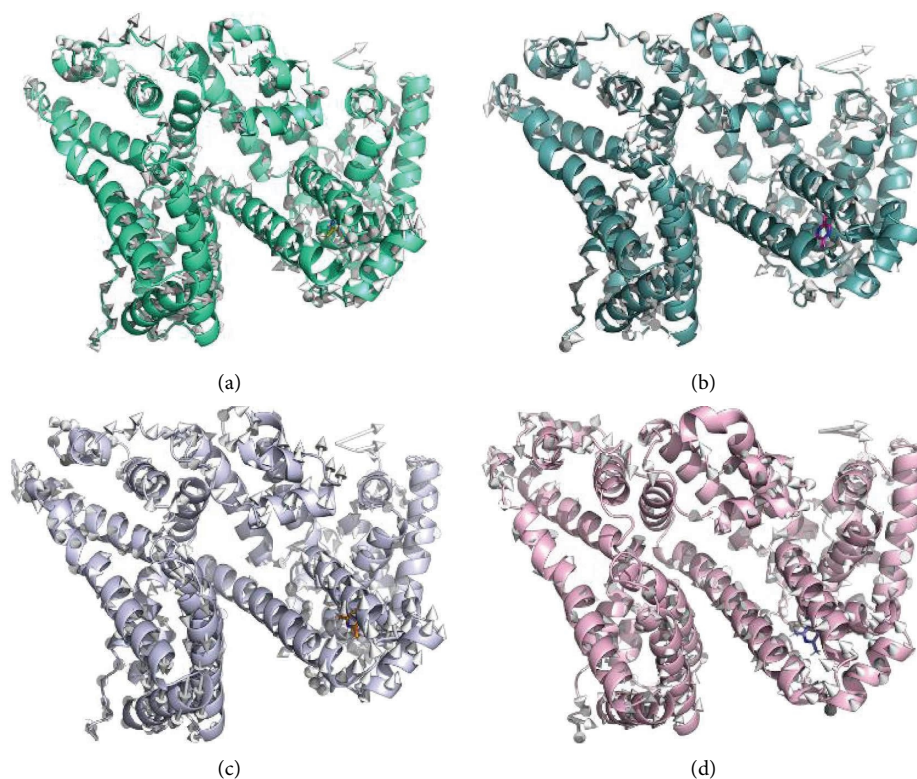

FIGURE 13: Conformational overlap before and after MD simulation (porcupine diagram): (a) 2,3-DMTP, (b) 2,5-DMTP, (c) TMTP, and (d) TTMP.

some hydrolyzed pNPA groups in its structure, resulting in reduced HSA esterase activity [57]. Among them, TTMP decreased the fastest, indicating that TTMP had the greatest effect on HSA esterase activity, which was related to the stability of TTMP and HSA binding.

Ellman's reagent can react with the thiol group of the free amino acid cysteine (Cys34) in HSA to form a yellow complex with a maximum absorption at 412 nm [58]. With the increase in the concentrations of 2,3-DMTP, 2,5-DMTP, and TMTP, the absorbance showed a downward trend
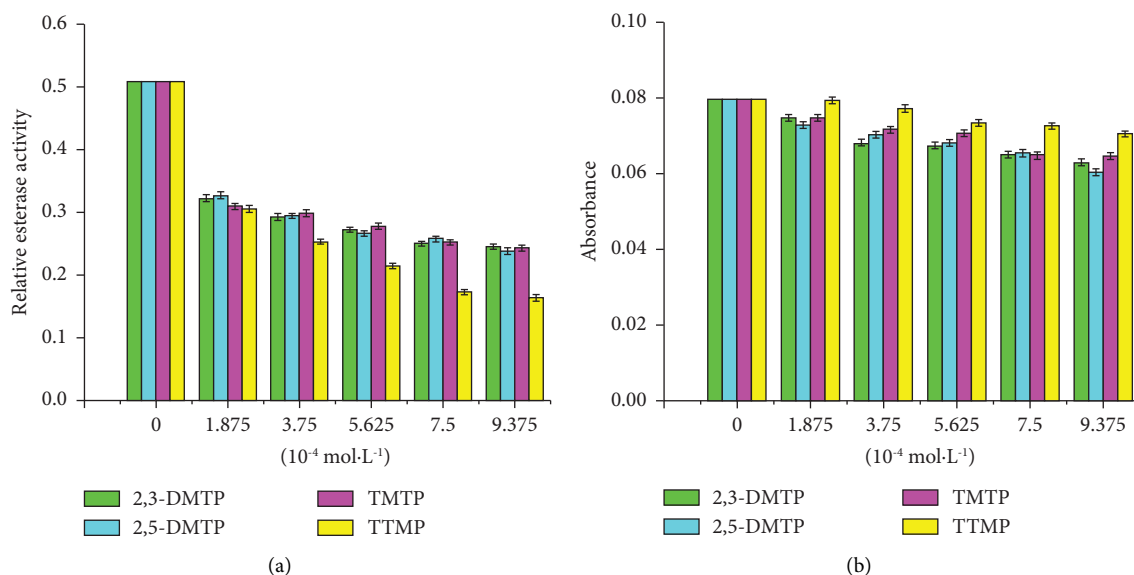
FIGURE 14: Effects of different substituted pyrazines on the physiological activity of HSA: (a) effects of different concentrations of pyrazine on the activity of HSA esterase and (b) effects of different concentrations of pyrazine on the free radical scavenging ability of HSA. $C_{HSA} = 1.0 \times 10^{-4}\,mol\,L^{-1}$ and $C_{2,3\text{-}DMTP} = C_{2,5\text{-}DMTP} = C_{TMTP} = C_{TTMP} = 1.875 \times 10^{-4}\,mol\cdot L^{-1}$.

(Figure 14(b)). It indicates that the interaction of 2,3-DMTP, 2,5-DMTP, and TMTP can reduce the radical scavenging capacity of HSA. The speculated reason for this may be that during the interaction between pyrazines and HSA, part of the active sites of HSA are occupied by small molecules of pyrazines, which makes it unable to combine with free radicals, thus reducing its antioxidant capacity. At the same time, the steric hindrance after combining with pyrazines is greater, which is not conducive to the free binding of HSA with free radicals [59, 60]. Contrary to the results of esterase activity, the free radical scavenging ability of HSA decreased only after TTMP reached a certain concentration, and TTMP had the least effect on the free radical scavenging ability of HSA.

4. Conclusions

This research employed the multispectral method and molecular dynamics simulation to investigate the interaction between different substituents of pyrazine and HSA. Binding constants, thermodynamic parameters, and molecular docking analysis showed that pyrazine mainly quenched the endogenous fluorescence of HSA through a static quenching mechanism. The hydrophobic force plays a major role in the binding of pyrazine compounds to HSA. According to Förster's nonradiative energy transfer theory, the binding distances of 2,3-DMTP, 2,5-DMTP, TTMP, and TMTP with HSA were calculated to be 2.99 nm, 2.82 nm, 3.49 nm, and 4.22 nm, respectively. The nonradiative energy transfer occurs between HSA and different pyrazines. The docking energy of different pyrazines with HSA is demonstrated as follows: TTMP > TMTP > 2,3-DMTP > 2,5-DMTP. It was between $-7.0\,kcal\cdot mol^{-1}$ and $-5.0\,kcal\cdot mol^{-1}$, indicating that HSA had good binding activity. Meanwhile, MD simulation results show that the combination of four pyrazines and HSA can enhance the stability of HSA. Among them, TTMP and HSA binding is the most stable, and TMTP is the most unstable combination with HSA. 2,3-DMTP and 2,5-DMTP have roughly the same effect on HSA stability. In addition, different pyrazines and HSA can reduce the esterase activity and free radical scavenging ability of HSA. It indicated that pyrazine could affect the physiological activity of HSA. Pyrazine compounds are widely used in food, spices, pharmaceuticals, and other industries. This paper deeply studies the interaction between pyrazines and HSA, which is helpful in understanding the reasons for the differences between pyrazines and protein functions in blood transport and in *in vivo* and *in vitro* biological activities, and provides a theoretical basis for the rational use of pyrazines and additives in food.

Data Availability

The data used to support the findings of this study are included within the article.

Conflicts of Interest

The authors declare that they have no conflicts of interest.

Authors' Contributions

Wenhua Tong and Shuqin Wang designed the study and wrote the manuscript. Zongwei Qiao and Ying Yang supervised the study and revised the manuscript. Wenhua Tong, Shuqin Wang, and Haoran Xu collected the data and visualized the study. Haoran Xu and Liming Zhao analyzed the data. All authors reviewed the manuscript and have read and approved the final version of the manuscript.

Acknowledgments

References

[1] M. M. Alam, F. Abul Qais, I. Ahmad, P. Alam, R. Hasan Khan, and I. Naseem, "Multi-spectroscopic and molecular modelling approach to investigate the interaction of riboflavin with human serum albumin," *Journal of Biomolecular Structure and Dynamics*, vol. 36, no. 3, pp. 795–809, 2018.

[2] S. Tayyab and S. R. Feroz, "Serum albumin: clinical significance of drug binding and development as drug delivery vehicle," *Advances in protein chemistry and structural biology*, vol. 123, pp. 193–218, 2021.

[3] R. R. Kudarha and K. K. Sawant, "Albumin based versatile multifunctional nanocarriers for cancer therapy: fabrication, surface modification, multimodal therapeutics and imaging approaches," *Materials Science and Engineering: C*, vol. 81, pp. 607–626, 2017.

[4] S. Zhu and Y. Liu, "Spectroscopic analyses on interaction of Naphazoline hydrochloride with bovine serum albumin," *Spectrochimica Acta Part A: Molecular and Biomolecular Spectroscopy*, vol. 98, pp. 142–147, 2012.

[5] M. K. Siddiqi, P. Alam, S. K. Chaturvedi, and R. H. Khan, "Anti-amyloidogenic behavior and interaction of diallylsulfide with human serum albumin," *International Journal of Biological Macromolecules*, vol. 92, pp. 1220–1228, 2016.

[6] H. Zhou, Z. Xiong, X. Ma et al., "A multispectral study and computer simulation on the interaction of pomalidomide with human serum albumin," *Journal of Molecular Liquids*, vol. 382, p. 121947, 2023.

[7] G. Melkonian, H. Eckelhoefer, M. Wu et al., "Growth and angiogenesis are inhibited in vivo in developing tissues by pyrazine and its derivatives," *Toxicological Sciences*, vol. 75, no. 2, pp. 393–401, 2003.

[8] F. B. Mortzfeld, C. Hashem, K. Vranková, M. Winkler, and F. Rudroff, "Pyrazines: synthesis and industrial application of these valuable flavor and fragrance compounds," *Biotechnology Journal*, vol. 15, no. 11, 2020.

[9] R. Müller and S. Rappert, "Pyrazines: occurrence, formation and biodegradation," *Applied Microbiology and Biotechnology*, vol. 85, no. 5, pp. 1315–1320, 2010.

[10] M. Qian and G. Reineccius, "Identification of aroma compounds in parmigiano-reggiano cheese by gas chromatography/olfactometry," *Journal of Dairy Science*, vol. 85, no. 6, pp. 1362–1369, 2002.

[11] R. Ascrizzi, G. Flamini, C. Tessieri, and L. Pistelli, "From the raw seed to chocolate: volatile profile of Blanco de Criollo in different phases of the processing chain," *Microchemical Journal*, vol. 133, pp. 474–479, 2017.

[12] F. Zamolo and M. Wüst, "3-Alkyl-2-Methoxypyrazines: overview of their occurrence, biosynthesis and distribution in edible plants," *ChemBioChem*, vol. 24, no. 19, Article ID e202300362, 2023.

[13] X. Wang, Y. Wang, G. Hu et al., "Review on factors affecting coffee volatiles: from seed to cup," *Journal of the Science of Food and Agriculture*, vol. 102, no. 4, pp. 1341–1352, 2022.

[14] X. Shi, S. Zhao, S. Chen et al., "Tetramethylpyrazine in Chinese baijiu: presence, analysis, formation, and regulation," *Frontiers in Nutrition*, vol. 9, Article ID 1004435, 2022.

[15] W. Zhang, G. Si, J. Li et al., "Tetramethylpyrazine in Chinese sesame flavour liquor and changes during the production process," *Journal of the Institute of Brewing*, vol. 125, no. 1, pp. 155–161, 2019.

[16] Z. Chen, C. Zhang, F. Gao et al., "A systematic review on the rhizome of Ligusticum chuanxiong Hort. (Chuanxiong)," *Food and Chemical Toxicology*, vol. 119, pp. 309–325, 2018.

[17] Y. Zhao, Y. Liu, and K. Chen, "Mechanisms and clinical application of tetramethylpyrazine (an interesting natural compound isolated from ligusticum wallichii): current status and perspective," *Oxidative Medicine and Cellular Longevity*, vol. 2016, Article ID 2124638, 9 pages, 2016.

[18] Y. J. Ma, J. H. Wu, X. Li et al., "Effect of alkyl distribution in pyrazine on pyrazine flavor release in bovine serum albumin solution," *Royal Society of Chemistry Advances*, vol. 9, no. 63, pp. 36951–36959, 2019.

[19] R. Bellam, D. Jaganyi, and R. S. Robinson, "Heterodinuclear Ru-Pt complexes bridged with 2,3-Bis(pyridyl)pyrazinyl ligands: studies on kinetics, deoxyribonucleic acid/bovine serum albumin binding and cleavage, in vitro cytotoxicity, and in vivo toxicity on zebrafish embryo activities," *American Chemical Society Omega*, vol. 7, no. 30, pp. 26226–26245, 2022.

[20] W. Hou, W. Dai, H. Huang et al., "Pharmacological activity and mechanism of pyrazines," *European Journal of Medicinal Chemistry*, vol. 258, Article ID 115544, 2023.

[21] G. De Simone, A. di Masi, and P. Ascenzi, "Serum albumin: a multifaced enzyme," *International Journal of Molecular Sciences*, vol. 22, no. 18, Article ID 10086, 2021.

[22] D. A. Belinskaia, P. A. Voronina, M. A. Vovk et al., "Esterase activity of serum albumin studied by 1H NMR spectroscopy and molecular modelling," *International Journal of Molecular Sciences*, vol. 22, no. 19, Article ID 10593, 2021.

[23] M. van de Weert and L. Stella, "Fluorescence quenching and ligand binding: a critical discussion of a popular methodology," *Journal of Molecular Structure*, vol. 998, no. 1-3, pp. 144–150, 2011.

[24] H. Mu, S. Chen, F. Liu et al., "Stereoselective interactions of lactic acid enantiomers with HSA: spectroscopy and docking application," *Food Chemistry*, vol. 270, pp. 429–435, 2019.

[25] H. Pu, H. Jiang, R. Chen, and H. Wang, "Studies on the interaction between vincamine and human serum albumin: a spectroscopic approach," *Luminescence*, vol. 29, no. 5, pp. 471–479, 2014.

[26] S. Seyedi, P. Parvin, A. Jafargholi et al., "Fluorescence emission quenching of RdB fluorophores in attendance of various blood type RBCs based on Stern-Volmer formalism," *Spectrochimica Acta Part A: Molecular and Biomolecular Spectroscopy*, vol. 248, Article ID 119237, 2021.

[27] L. Zhu, X. Song, F. Pan et al., "Interaction mechanism of kafirin with ferulic acid and tetramethyl pyrazine: multiple spectroscopic and molecular modeling studies," *Food Chemistry*, vol. 363, Article ID 130298, 2021.

[28] M. S. H. Akash and K. Rehman, "Ultraviolet-visible (UV-VIS) spectroscopy," *Essentials of Pharmaceutical Analysis*, pp. 29–56, 2020.

[29] M. Iosin, F. Toderas, P. L. Baldeck, and S. Astilean, "Study of protein–gold nanoparticle conjugates by fluorescence and surface-enhanced Raman scattering," *Journal of Molecular Structure*, vol. 924, pp. 196–200, 2009.

[30] N. Nagano, M. Ota, and K. Nishikawa, "Strong hydrophobic nature of cysteine residues in proteins," *Federation of European Biochemical Societies Letters*, vol. 458, no. 1, pp. 69–71, 1999.

[31] F. Poureshghi, P. Ghandforoushan, A. Safarnejad, and S. Soltani, "Interaction of an antiepileptic drug, lamotrigine with human serum albumin (HSA): application of spectroscopic techniques and molecular modeling methods," *Journal of Photochemistry and Photobiology B: Biology*, vol. 166, pp. 187–192, 2017.

[32] S. Rahman, M. T. Rehman, G. Rabbani et al., "Insight of the interaction between 2,4-thiazolidinedione and human serum albumin: a spectroscopic, thermodynamic and molecular docking study," *International Journal of Molecular Sciences*, vol. 20, no. 11, p. 2727, 2019.

[33] V. Hornok, Á. Juhász, G. Paragi, A. N. Kovács, and E. Csapó, "Thermodynamic and kinetic insights into the interaction of kynurenic acid with human serum albumin: spectroscopic and calorimetric approaches," *Journal of Molecular Liquids*, vol. 313, Article ID 112869, 2020.

[34] S. Tang, J. Li, G. Huang, and L. Yan, "Predicting protein surface property with its surface hydrophobicity," *Protein and Peptide Letters*, vol. 28, no. 8, pp. 938–944, 2021.

[35] S. Sarzehi and J. Chamani, "Investigation on the interaction between tamoxifen and human holo-transferrin: determination of the binding mechanism by fluorescence quenching, resonance light scattering and circular dichroism methods," *International Journal of Biological Macromolecules*, vol. 47, no. 4, pp. 558–569, 2010.

[36] Q. Fang, C. Guo, Y. Wang, and Y. Liu, "The study on interactions between levofloxacin and model proteins by using multi-spectroscopic and molecular docking methods," *Journal of Biomolecular Structure and Dynamics*, vol. 36, no. 8, pp. 2032–2044, 2018.

[37] J. Liang, Y. Cheng, and H. Han, "Study on the interaction between bovine serum albumin and CdTe quantum dots with spectroscopic techniques," *Journal of Molecular Structure*, vol. 892, no. 1-3, pp. 116–120, 2008.

[38] A. Zamora-Gálvez, E. Morales-Narváez, J. Romero, and A. Merkoçi, "Photoluminescent lateral flow based on non-radiative energy transfer for protein detection in human serum," *Biosensors and Bioelectronics*, vol. 100, pp. 208–213, 2018.

[39] G. Ren, H. Sun, J. Guo, J. Fan, G. Li, and S. Xu, "Molecular mechanism of the interaction between resveratrol and trypsin via spectroscopy and molecular docking," *Food and Function*, vol. 10, no. 6, pp. 3291–3302, 2019.

[40] N. Shahabadi and S. Zendehcheshm, "Evaluation of ct-DNA and HSA binding propensity of antibacterial drug chloroxine: multi-spectroscopic analysis, atomic force microscopy and docking simulation," *Spectrochimica Acta Part A: Molecular and Biomolecular Spectroscopy*, vol. 230, Article ID 118042, 2020.

[41] I. Singh, V. Luxami, and K. Paul, "Spectroscopy and molecular docking approach for investigation on the binding of nocodazole to human serum albumin," *Spectrochimica Acta Part A: Molecular and Biomolecular Spectroscopy*, vol. 235, Article ID 118289, 2020.

[42] A. S. Tatikolov and S. M. Costa, "Complexation of polymethine dyes with human serum albumin: a spectroscopic study," *Biophysical Chemistry*, vol. 107, no. 1, pp. 33–49, 2004.

[43] F. S. Mohseni-Shahri, F. Moeinpour, and M. Nosrati, "Spectroscopy and molecular dynamics simulation study on the interaction of sunset yellow food additive with pepsin," *International Journal of Biological Macromolecules*, vol. 115, pp. 273–280, 2018.

[44] G. Magdy, M. A. Shaldam, F. Belal, and H. Elmansi, "Multi-spectroscopic, thermodynamic, and molecular docking/dynamic approaches for characterization of the binding interaction between calf thymus DNA and palbociclib," *Scientific Reports*, vol. 12, no. 1, Article ID 14723, 2022.

[45] B. Lorber, F. Fischer, M. Bailly, H. Roy, and D. Kern, "Protein analysis by dynamic light scattering: methods and techniques for students," *Biochemistry and Molecular Biology Education*, vol. 40, no. 6, pp. 372–382, 2012.

[46] M. Bolattin, S. Nandibewoor, S. Joshi, S. Dixit, and S. Chimatadar, "Interaction of hydralazine with human serum albumin and effect of β-cyclodextrin on binding: insights from spectroscopic and molecular docking techniques," *Industrial and Engineering Chemistry Research*, vol. 55, no. 19, pp. 5454–5464, 2016.

[47] X. Tao, Y. Huang, C. Wang et al., "Recent developments in molecular docking technology applied in food science: a review," *International Journal of Food Science and Technology*, vol. 55, no. 1, pp. 33–45, 2019.

[48] R. Patel, B. Singh, A. Sharma et al., "Interaction and esterase activity of albumin serums with orphenadrine: a spectroscopic and computational approach," *Journal of Molecular Structure*, vol. 1239, Article ID 130522, 2021.

[49] B. K. Kundu, Pragti, S. M. Mobin, and S. Mukhopadhyay, "Studies on the influence of the nuclearity of zinc(ii) hemisalen complexes on some pivotal biological applications," *Dalton Transactions*, vol. 49, no. 43, pp. 15481–15503, 2020.

[50] J. F. Fatriansyah, R. K. Rizqillah, M. Y. Yandi, Fadilah, and M. Sahlan, "Molecular docking and dynamics studies on propolis sulabiroin-A as a potential inhibitor of SARS-CoV-2," *Journal of King Saud University Science*, vol. 34, no. 1, Article ID 101707, 2022.

[51] A. Grossfield, S. E. Feller, and M. C. Pitman, "Convergence of molecular dynamics simulations of membrane proteins," *Proteins: Structure, Function, and Bioinformatics*, vol. 67, no. 1, pp. 31–40, 2007.

[52] R. Saxena, S. K. Vanga, and V. Raghavan, "Effect of thermal and microwave processing on secondary structure of bovine β-lactoglobulin: a molecular modeling study," *Journal of Food Biochemistry*, vol. 43, no. 7, Article ID e12898, 2019.

[53] F. Zhan, S. Ding, W. Xie et al., "Towards understanding the interaction of β-lactoglobulin with capsaicin: multi-spectroscopic, thermodynamic, molecular docking and molecular dynamics simulation approaches," *Food Hydrocolloids*, vol. 105, Article ID 105767, 2020.

[54] J. Mittal and R. B. Best, "Thermodynamics and kinetics of protein folding under confinement," *Proceedings of the National Academy of Sciences*, vol. 105, no. 51, pp. 20233–20238, 2008.

[55] S. A. Ali, M. I. Hassan, A. Islam, and F. Ahmad, "A review of methods available to estimate solvent-accessible surface areas of soluble proteins in the folded and unfolded states," *Current Protein and Peptide Science*, vol. 15, no. 5, pp. 456–476, 2014.

[56] X. Hu, W. Song, W. Li, C. Guo, Z. Yu, and R. Liu, "Effects of γ-irradiation on the molecular structures and functions of human serum albumin," *Journal of Biochemical and Molecular Toxicology*, vol. 30, no. 11, pp. 525–532, 2016.

[57] C. N. Patel, S. P. Kumar, H. A. Pandya, and R. M. Rawal, "Identification of potential inhibitors of coronavirus hemagglutinin-esterase using molecular docking, molecular dynamics simulation and binding free energy calculation," *Molecular Diversity*, vol. 25, no. 1, pp. 421–433, 2021.

[58] S. Arfin, G. A. Siddiqui, A. Naeem, and S. Moin, "Inhibition of advanced glycation end products by isoferulic acid and its free radical scavenging capacity: an in vitro and molecular docking study," *International Journal of Biological Macromolecules*, vol. 118, no. Pt B, pp. 1479–1487, 2018.

[59] Y. Ying, S. Wang, X. Liu et al., "Interactions of ferulic acid and ferulic acid methyl ester with endogenous proteins: determination using the multi-methods," *Heliyon*, vol. 10, no. 2.

[60] N. Maurya, J. K. Maurya, U. K. Singh et al., "In vitro cytotoxicity and interaction of noscapine with human serum albumin: effect on structure and esterase activity of HSA," *Molecular Pharmaceutics*, vol. 16, no. 3, pp. 952–966, 2019.